IET Research Journals

Submission Template for IET Research Journal Papers

IET Journals
The Institution of Engineering and Technology

Optimising Coverage Efficiency in Heterogeneous Wireless Cellular Networks

ISSN 1751-8644
doi: 0000000000
www.ietdl.org

Ca V. Phan[1] *and Quoc-Tuan Vien*[2]

[1] *Faculty of Electrical and Electronics Engineering, Ho Chi Minh City University of Technology and Education, Vietnam. * E-mail: capv@hcmute.edu.vn.*
[2] *Faculty of Science and Technology, Middlesex University, The Burroughs, London, United Kingdom.* E-mail: Q.Vien@mdx.ac.uk*

Abstract: In this study, the authors first propose an analytical model for investigating the impacts of power allocation (PA) and cell density allocation (CDA) on coverage efficiency (CE) of heterogeneous wireless cellular networks (HWCNs) under limited resources. It is shown that the interference among cells that belong to different tiers is reduced significantly in higher path loss environment and results in a higher coverage. The network coverage of the HWCN can be further extended with the deployment of a higher cell density in a more lossy environment. This accordingly leads us to develop an optimisation problem (OP) to maximise the CE by optimising the PA and CDA under the constraint of limited cell power and total power available in the downlink HWCN. In particular, they proposed a two-stage approach for solving the OP to sequentially obtain the heuristic value of the CDA and PA due to complicated objective function along with various involved parameters. Numerical results reveal that the coverage obtained by the heuristic solution at the first-stage is significantly improved with lower power than the conventional approach. Furthermore, an enhanced overall CE is achieved for all cases of the power constraint when applying fully two stages in their proposed algorithm.

1 Introduction

Heterogeneous wireless cellular networks (HWCNs) have attracted a tremendous number of research to cope with the persistent increase of the number of mobile users in 5G and beyond networks [1–5]. By combining networks of different sizes with distinct characteristics, such as macrocells, microcells, picocells, femtocells [6–12], etc., the HWCN are regarded as a generalised model of the future networks. Such mixture of cells has been promising to enhance not only the network coverage but also the network capacity aiming at providing the best quality-of-service (QoS) for all mobile users regardless of their geographical location. The HWCNs with multiple overlaying layers, a.k.a. tiers, have indeed been shown to improve the QoS of both indoor and outdoor users along with an extensive coverage for cell-edge users.

Although HWCNs have been well devised and theoretically analysed, the employment of a variety of cells in practice raises several concerns among which the critical issue is the resource management due to the interferences between these cells of either the same or different types. An increased power level at a cell can enhance the performance of users located within it; however, this causes cross-tier interferences to other cells, which may degrade their performance. A resource allocation mechanism is therefore vital in the practical HWCNs. Specifically, various power control mechanisms were proposed in [13–18] to mitigate the interferences in the HWCNs.

Considering large-scale wireless networks, signal-to-interference-plus-noise ratio (SINR) is generally intractable with random user location, variant cell size, user density, cell density and changing propagation environment. Dealing with this, stochastic geometry has been adopted for modelling cellular networks to reflect the practical cellular networks with tractable analytical results of various performance metrics, such as coverage and rate [19–21]. The stochastic geometry has been shown to yield accurate performance bounds in the HWCNs to capture the randomness of the networks with variant topologies in practice [22–25], and thus it has been extensively investigated in the literature for modelling and analyses of various HWCNs, such as the work in [2, 20, 26].

In [27], the employment of almost blank subframe for cell range expansion and idle mode capability of base stations (BSs) was proposed to mitigate the under-utilisation of small BSs. By switching off the transmission modules of the unused BSs when there is no active user equipments (UEs) within their designated coverage area, the wasted energy consumption can be remarkably reduced, while the active UEs can be associated and still can be covered by the remaining BSs. An enhanced coverage is even achieved as a result of the reduction of the interference caused by the unused BSs. In [28], a dynamic sleeping strategy was proposed, which allows the cell densities to be changed to optimise energy efficiency. Another sleeping technique was also developed in [29] where sleep mode for energy efficiency and cell range expansion technique for enhanced coverage area are incorporated.

In general both power and cell densities are shown to have considerable impacts on the coverage probability (CP) of an HWCN. The optimisation of the CP is therefore vital in the practical HWCNs where various aspects of the propagation environment within different cells along with the limited resource need to be taken into account. Although the problem of resource allocation for the HWCNs has been well studied in the literature with a variety of approaches, the actual coverage is still restricted due to the fact that optimising the transmission power of BSs with high cell density does not necessarily lead to a higher coverage. This accordingly motivates us to investigate the efficiency of both the power allocation (PA) and cell density allocation (CDA) on the coverage of the practical HWCNs.

In this paper, we first analyse the impacts of PA and CDA on the CP of an HWCN taking into account various propagation environment. With the aim of maximising the coverage with a minimal power consumption, we then develop an optimisation problem (OP) for the resource allocation in the HWCN. The main contributions of this paper can be summarised as follows:

- Coverage efficiency (CE) of a downlink HWCN is analysed taking into account the impact of propagation environment on the CP. Specifically, it is shown that, in an environment experiencing higher path loss, the interference caused by the cells of different tiers is reduced significantly, which accordingly results in a higher CP. Moreover, the coverage of the HWCN can be further enhanced with the deployment of a higher cell density in a more lossy environment rather than in a less lossy one; meanwhile, the additive white Gaussian noise (AWGN) in conventional communication channels

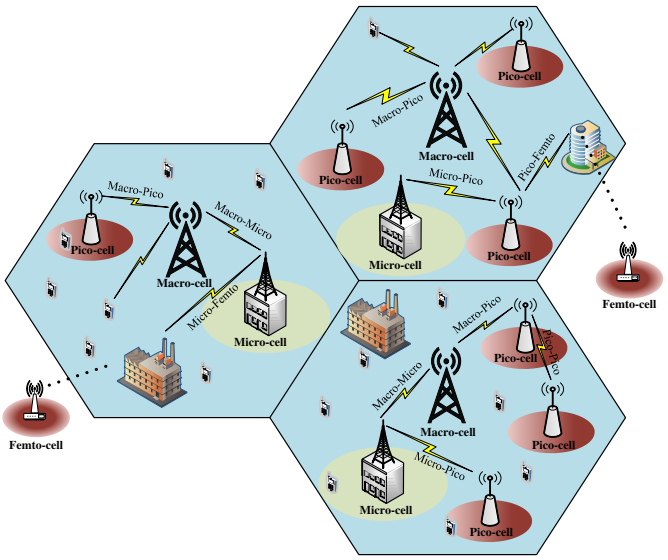

Fig. 1: System model of an HWCN.

is shown to have not much effect on the coverage given the dominant interference of different cells in the HWCN. The PA and CDA therefore have remarkable impacts on the CE of the practical HWCN.

- An OP is proposed to find the optimal PA and CDA that maximise CE in an HWCN subject to the constraint of limited power at cells and total power available in the network. It is shown that the OP is hard to be directly solved owing to a complicated objective function along with various involved parameters in the practical HWCN.
- A two-stage approach is designed to sequentially find optimal CDA and PA so as to maximise the CE. In the first stage, the optimal CDA for maximising the coverage area in the practical HWCN is identified, while the PA is solved in the second stage subject to a minimum coverage requirement. The first stage is shown to provide an enhanced coverage with a lower power consumption compared to the equal CDA approach. In addition, the PA in the second stage can help reduce the total power consumption further to maximise the CE.

The rest of this paper is organised as follows: Section II describes the system model of a practical HWCN. The CE of the HWCN is derived in Section III, followed by the proposal of the optimisation problem for maximising the CE in Section IV. Sections V and VI sequentially present two stages for finding optimal CDA and PA in the HWCN. Numerical results are presented in Section VII to validate the findings. Finally, Section VIII draws the main conclusions of the work.

2 System Model of a Practical HWCN

Figure 1 illustrates the system model of an HWCN consisting of K tiers of BSs. Each tier can be either macrocell, picocell or microcell depending on its transmission power and density in the network. Taking into account the practical environment, it is assumed that there are totally L different propagation models, each of which is represented by a path loss exponent α_l, $l = 1, 2, \ldots, L$,* and the number of models in the k-th tier, $k = 1, 2, \ldots, K$, is $L_k \leq L$. The number of BSs in the k-th tier is modeled by a Poisson point process (PPP), namely Φ_k, having a cell density of λ_k. The transmission power of the BS in the k-th tier is denoted by P_k.

It is noticed that the BSs in the same tier may experience different propagation environment, and thus they should adjust their transmission power and their density may also vary. Specifically, in the k-th tier, $k = 1, 2, \ldots, K$, let us assume the number of BSs experiencing the i_k-th propagation environment, $i_k = 1, 2, \ldots, L_k$, is independently distributed following a thinning PPP $\Phi_{k,i_k} \subset \Phi_k$ with density λ_{k,i_k}. The transmission power of these BSs is accordingly set as P_{k,i_k}, which is limited by $P_{k,i_k} \leq P_k, \forall i_k = 1, 2, \ldots, L_k$.†

Let us consider the downlink from a BS to a mobile station (MS) located at a point x_{k,i_k} within the (k, i_k)-th model, $k = 1, 2, \ldots, K$, $i_k = 1, 2, \ldots, L_k$. The data communication of the downlink is assumed to experience Rayleigh flat fading with channel coefficient of h_{k,i_k} which is exponentially distributed, i.e. $h_{k,i_k} \sim \text{Exp}(1)$. The downlink SINR at the MS, denoted by γ_{k,i_k}, can be determined by

$$\gamma_{k,i_k} = \frac{P_{k,i_k} h_{k,i_k} \|x_{k,i_k}\|^{-\alpha_{i_k}}}{\sum_{m=1}^{K} \sum_{i_m=1}^{L_m} \sum_{x \in \Phi_{m,i_m} \setminus x_{k,i_k}} P_{m,i_m} h_x \|x\|^{-\alpha_{i_m}} + N_0}, \tag{1}$$

where N_0 is the noise power in AWGN model and $\|\cdot\|$ denotes Euclidean norm operator.

For simplicity, let us denote the cumulative interference from all propagation environment models in all tiers when the MS is at x_{k,i_k}, $k = 1, 2, \ldots, K$, $i_k = 1, 2, \ldots, L_k$, by

$$I_{k,i_k} \triangleq \sum_{m=1}^{K} \sum_{i_m=1}^{L_m} \sum_{x \in \Phi_{m,i_m} \setminus x_{k,i_k}} P_{m,i_m} h_x \|x\|^{-\alpha_{i_m}}. \tag{2}$$

The downlink SINR γ_{k,i_k} in (1) can be rewritten as

$$\gamma_{k,i_k} = \frac{P_{k,i_k} h_{k,i_k} \|x_{k,i_k}\|^{-\alpha_{i_k}}}{I_{k,i_k} + N_0}. \tag{3}$$

In order to reliably send data from BS to MS, the downlink SINR is required to be not lower than an SINR threshold. Letting $\bar{\gamma}_k$, $k = 1, 2, \ldots, K$ denote the SINR threshold over the downlink in the k-th tier, the condition for maintaining the coverage of a MS located at x_{k,i_k}, $i_k = 1, 2, \ldots, L_k$, is thus expressed by:

$$\gamma_{k,i_k} \geq \bar{\gamma}_k. \tag{4}$$

Given various requirements in the HWCN with different SINR thresholds at the MS, i.e. $\bar{\gamma}_k$, $k = 1, 2, \ldots, K$ and limited transmission power at the BS, i.e. P_k, the coverage should be maximised in an efficient way with the least total power consumption in the whole network.

For convenience, notations used throughout the paper are summarised in Table 1 in chronological order of their appearances.

3 Coverage Efficiency in an HWCN

Intuitively, increasing transmission power of BS helps enhance its own coverage. However, this fact is not always true in a practical HWCN where such increased power may cause interferences to the neighbouring cells and, as a consequence, it even reduces the coverage of the whole network. This accordingly motivates us to investigate CE metric which is defined as the percentage of area that can be covered with a unit of power.

The path loss exponent is practically determined based on experimental measurement in different indoor and outdoor propagation environment.

†*For brevity in presentation, the 2-tuple (k, i_k) is used throughout the paper to denote the k-th tier and the i_k-th propagation environment, respectively, unless otherwise stated.*

Table 1 Summary of notations

Notation	Meaning
K	number of tiers
L	total number of propagation models
L_k	number of propagation models in the k-th tier
α_l	path loss exponent of the l-th propagation model
Φ_k	PPP model of the number of BSs in the k-th tier
λ_k	cell density of the PPP Φ_k
(k, i_k)	i_k-th propagation environment in the k-th tier
Φ_{k,i_k}	PPP model of the number of BSs in the (k, i_k)-th model
λ_{k,i_k}	cell density of the PPP Φ_{k,i_k}
P_k	transmission power of BSs in the k-th tier
P_{k,i_k}	transmission power of a BS within the (k, i_k)-th model
x_{k,i_k}	location of a MS within the (k, i_k)-th model
h_{k,i_k}	channel coefficient within the (k, i_k)-th model
γ_{k,i_k}	SINR at a MS within the (k, i_k)-th model
N_0	noise power in AWGN model
$\|\cdot\|$	Euclidean norm operator
I_{k,i_k}	cumulative interference at a MS within the (k, i_k)-th model
$\bar{\gamma}_k$	SINR threshold in the k-th tier
$\mathcal{P}_C$	CP of an HWCN
P_T	total power consumption in an HWCN
ζ	CE of an HWCN
$\mathbb{P}[X]$	probability of X
$\bigcup_i \mathfrak{S}_i$	union of a set collection $\{\mathfrak{S}_i\}$
$E[X]$	statistical expectation of X
$\mathcal{L}[\cdot]$	Laplace transform

Let ζ, $\mathcal{P}_C$ and P_T denote the CE, CP and total power consumption, respectively, in an HWCN. By definition, ζ can be given by

$$\zeta \triangleq \frac{\mathcal{P}_C}{P_T}, \tag{5}$$

where P_T is computed by considering the power consumption of all BSs in the HWCN, i.e.

$$P_T = \sum_{k=1}^{K} \sum_{i_k=1}^{L_k} \lambda_{k,i_k} P_{k,i_k}, \tag{6}$$

and $\mathcal{P}_C$ is determined from the condition of coverage (see (4)) by

$$\mathcal{P}_C \triangleq \mathbb{P}\left[\bigcup_{\substack{1\le k\le K \\ 1\le i_k\le L_k \\ x_{k,i_k}\in\Phi_{k,i_k}}} \gamma_{k,i_k} > \bar{\gamma}_k \right]. \tag{7}$$

Here, $\mathbb{P}[X]$ and $\bigcup_i \mathfrak{S}_i$ denote the probability of a random variable X and the union of a set collection $\{\mathfrak{S}_i\}$, respectively.

We have the following finding:

Theorem 1. *The CE of a practical HWCN can be obtained by*

$$\begin{aligned}\zeta =& \frac{1}{\sum_{k=1}^{K}\sum_{i_k=1}^{L_k}\lambda_{k,i_k}P_{k,i_k}} \sum_{k=1}^{K}\sum_{i_k=1}^{L_k}\lambda_{k,i_k} \\ &\times \int_{\mathbb{R}^2} \exp\left(-\frac{\bar{\gamma}_k N_0}{P_{k,i_k}}\|x_{k,i_k}\|^{\alpha_{i_k}}\right) \prod_{m=1}^{K}\prod_{i_m=1}^{L_m} \exp\Big[-2\pi^2 \\ &\times \frac{\csc\left(\frac{2\pi}{\alpha_{i_m}}\right)}{\alpha_{i_m}} \bar{\gamma}_k^{\frac{2}{\alpha_{i_m}}} \lambda_{m,i_m} \left(\frac{P_{m,i_m}}{P_{k,i_k}}\right)^{\frac{2}{\alpha_{i_m}}}\Big] dx_{k,i_k}.\end{aligned} \tag{8}$$

Proof: Firstly, let us analyse the CP of a practical HWCN. From (7), $\mathcal{P}_C$ with downlink SINR connectivity model can be derived as

$$\begin{aligned}\mathcal{P}_C &\overset{(a)}{=} E\left[\mathbf{1}\left(\bigcup_{\substack{1\le k\le K \\ 1\le i_k\le L_k \\ x_{k,i_k}\in\Phi_{k,i_k}}} \gamma_{k,i_k} > \bar{\gamma}_k\right)\right] \\ &\overset{(b)}{=} \sum_{k=1}^{K}\sum_{i_k=1}^{L_k} E\left[\sum_{x_{k,i_k}\in\Phi_{k,i_k}} \mathbf{1}\left(\gamma_{k,i_k} > \bar{\gamma}_k\right)\right] \\ &\overset{(c)}{=} \sum_{k=1}^{K}\sum_{i_k=1}^{L_k} E\left[\sum_{x_{k,i_k}\in\Phi_{k,i_k}} \mathbf{1}\left(\frac{P_{k,i_k}h_{k,i_k}\|x_{k,i_k}\|^{-\alpha_{i_k}}}{I_{k,i_k}+N_0} > \bar{\gamma}_k\right)\right] \\ &\overset{(d)}{=} \sum_{k=1}^{K}\sum_{i_k=1}^{L_k} \lambda_{k,i_k}\int_{\mathbb{R}^2} \mathbb{P}\left(\frac{P_{k,i_k}h_{k,i_k}\|x_{k,i_k}\|^{-\alpha_{i_k}}}{I_{k,i_k}+N_0} > \bar{\gamma}_k\right) dx_{k,i_k},\end{aligned} \tag{9}$$

where $E[X]$ denotes the statistical expectation of random variable X, (a) is due to the definition of the truth set in (7), (b) is owing to the assumption of disjoint union set of coverage area over different propagation environment, (c) is obtained by substituting (3) into (9) and (d) is followed by applying Campbell Mecke Theorem as in [26].

For simplicity, let us define

$$\Theta_{k,i_k} \triangleq \mathbb{P}\left(\frac{P_{k,i_k}h_{k,i_k}\|x_{k,i_k}\|^{-\alpha_{i_k}}}{I_{k,i_k}+N_0} > \bar{\gamma}_k\right). \tag{10}$$

The CP in (9) can be obtained by deriving Θ_{k,i_k} as follows:

$$\begin{aligned}\Theta_{k,i_k} &= \mathbb{P}\left[h_{k,i_k} > \frac{\bar{\gamma}_k\|x_{k,i_k}\|^{\alpha_{i_k}}}{P_{k,i_k}}\left(I_{k,i_k}+N_0\right)\right] \\ &= E_{I_{k,i_k}}\left[\mathbb{P}\left(h_{k,i_k} > \frac{\bar{\gamma}_k\|x_{k,i_k}\|^{\alpha_{i_k}}}{P_{k,i_k}}\left(I_{k,i_k}+N_0\right)\middle| I_{k,i_k}\right)\right] \\ &\overset{(a)}{=} E_{I_{k,i_k}}\left[\exp\left(-\frac{\bar{\gamma}_k\|x_{k,i}\|^{\alpha_{k,i}}}{P_{k,i_k}}\left(I_{k,i_k}+N_0\right)\right)\right] \\ &\overset{(b)}{=} \exp\left(-\frac{\bar{\gamma}_k N_0}{P_{k,i_k}}\|x_{k,i_k}\|^{\alpha_{i_k}}\right)\mathcal{L}_{I_{k,i_k}}\left[\frac{\bar{\gamma}_k}{P_{k,i_k}}\|x_{k,i_k}\|^{\alpha_{i_k}}\right],\end{aligned} \tag{11}$$

where (a) is due to the assumption $h_{k,i_k} \sim \text{Exp}(1)$, $k = 1, 2, \ldots, K$, $i_k = 1, 2, \ldots, L_k$, and (b) is obtained by the Laplace transform, i.e. $\mathcal{L}[\cdot]$. The derivation of Θ_{k,i_k} can be thus deduced

$$\mathcal{P}_C = \sum_{k=1}^{K}\sum_{i_k=1}^{L_k} \lambda_{k,i_k} \int_{\mathbb{R}^2} \exp\left(-\frac{\bar{\gamma}_k N_0}{P_{k,i_k}}\|x_{k,i_k}\|^{\alpha_{i_k}}\right) \prod_{m=1}^{K}\prod_{i_m=1}^{L_m} \exp\left[-2\pi^2 \frac{\csc\left(\frac{2\pi}{\alpha_{i_m}}\right)}{\alpha_{i_m}} \bar{\gamma}_k^{\frac{2}{\alpha_{i_m}}} \lambda_{m,i_m} \left(\frac{P_{m,i_m}}{P_{k,i_k}}\right)^{\frac{2}{\alpha_{i_m}}}\right] dx_{k,i_k}. \quad (13)$$

from the computation of $\mathcal{L}_{I_{k,i_k}}[s]$ as in the following steps:

$$\begin{aligned}
\mathcal{L}_{I_{k,i_k}}[s] &= E_{I_{k,i_k}}\left[\exp\left(-sI_{k,i_k}\right)\right] \\
&\overset{(a)}{=} E_{I_{k,i_k}}\left[\exp\left(-s\sum_{m=1}^{K}\sum_{i_m=1}^{L_m}\sum_{x\in\Phi_{m,i_m}\setminus x_{k,i_k}} P_{m,i_m} h_x \|x\|^{-\alpha_{i_m}}\right)\right] \\
&= \prod_{m=1}^{K}\prod_{i_m=1}^{L_m} E_{I_{k,i_k}}\left[\prod_{x\in\Phi_{m,i_m}\setminus x_{k,i_k}} \exp\left(-sP_{m,i_m} h_x \|x\|^{-\alpha_{i_m}}\right)\right] \\
&\overset{(b)}{=} \prod_{m=1}^{K}\prod_{i_m=1}^{L_m} E_{\Phi_{m,i_m}}\left[\prod_{x\in\Phi_{m,i_m}\setminus x_{k,i_k}} E_{h_x}\left[\exp\left(-sP_{m,i_m} \times h_x\|x\|^{-\alpha_{i_m}}\right)\right]\right] \\
&\overset{(c)}{=} \prod_{m=1}^{K}\prod_{i_m=1}^{L_m} E_{\Phi_{m,i_m}}\left[\prod_{x\in\Phi_{m,i_m}\setminus x_{k,i_k}} \frac{1}{1+sP_{m,i_m}\|x\|^{-\alpha_{i_m}}}\right] \\
&\overset{(d)}{=} \prod_{m=1}^{K}\prod_{i_m=1}^{L_m} \exp\left[-\lambda_{m,i_m} \times \int_{\mathbb{R}^2}\left(1-\frac{1}{1+sP_{m,i_m}\|x\|^{-\alpha_{i_m}}}\right)dx\right] \\
&\overset{(e)}{=} \prod_{m=1}^{K}\prod_{i_m=1}^{L_m} \exp\left[-\lambda_{m,i_m} \times \int_0^{2\pi}\int_0^{\infty}\left(1-\frac{1}{1+sP_{m,i_m} r^{-\alpha_{i_m}}}\right) r dr d\theta\right] \\
&= \prod_{m=1}^{K}\prod_{i_m=1}^{L_m} \exp\left[-2\pi\lambda_{m,i_m}\int_0^{\infty}\frac{sP_{m,i_m} r^{1-\alpha_{i_m}}}{1+sP_{m,i_m} r^{-\alpha_{i_m}}} dr\right] \\
&\overset{(f)}{=} \prod_{m=1}^{K}\prod_{i_m=1}^{L_m} \exp\left[-2\pi^2 \frac{\lambda_{m,i_m}}{\alpha_{i_m}} \left(sP_{m,i_m}\right)^{\frac{2}{\alpha_{i_m}}} \csc\left(\frac{2\pi}{\alpha_{i_m}}\right)\right],
\end{aligned} \quad (12)$$

where (a) is given by the definition of interference at a mobile user (see (2)), (b) is due to the fact that random variables in $\{I_{k,i_k}\}$ are independent, (c) follows from the assumption $h_x \sim \text{Exp}(1)$, (d) is obtained by applying the probability generating functional of a PPP [24] (i.e. $E_\Phi[\prod_{x\in\Phi} f(x)] = \exp[-\lambda \int_{\mathbb{R}^2}(1-f(x))dx]$), (e) is computed by converting from Cartesian to polar coordinates and (f) is obtained by using [30, eq. (3.241.2)].

Replacing s in (12) by $\frac{\bar{\gamma}_k}{P_{k,i_k}}\|x_{k,i_k}\|^{\alpha_{i_k}}$ into (11), Θ_{k,i_k} can be derived, and thus the CP in (9) can be deduced as in (13) (see the top of next page).

Substituting (13) into (5) with the total power consumption given by (6), we obtain the CE as in (8). This completes the proof. □

Lemma 1. *Considering heterogeneous propagation media with equal cell density and equal power allocation of BSs in set $\{\Phi_{k,i_k}\}$, $k = 1, 2, \ldots, K$, $i_k = 1, 2, \ldots, L_k$, the CE of a HWCN can be obtained by*

$$\begin{aligned}
\zeta = &\frac{1}{\sum_{k=1}^{K}\lambda_k P_k}\sum_{k=1}^{K}\frac{\lambda_k}{L_k}\sum_{i_k=1}^{L_k}\int_{\mathbb{R}^2} e^{-\frac{\bar{\gamma}_k N_0}{P_k}\|x_{k,i_k}\|^{\alpha_{i_k}}} \\
&\times \exp\left[-2\pi^2\sum_{m=1}^{K}\frac{\lambda_m}{L_m}\sum_{i_m=1}^{L_m}\frac{\csc\left(\frac{2\pi}{\alpha_{i_m}}\right)}{\alpha_{i_m}}\left(\bar{\gamma}_k\frac{P_m}{P_k}\right)^{\frac{2}{\alpha_{i_m}}}\right] dx_{k,i_k}.
\end{aligned} \quad (14)$$

Proof: With equal cell density and transmission power in each tier regardless of the propagation environment, we have $\lambda_{k,i_1} = \lambda_{k,i_2} = \cdots = \lambda_{k,L_k} = \lambda_k/L_k$ and $P_{k,i_1} = P_{k,i_2} = \cdots = P_{k,L_k} = P_k$, where $k = 1, 2, \ldots, K$. Substituting into (8) with some manipulations, we can arrive at (14). This completes the proof. □

Corollary 1. *Considering homogeneous propagation media in each tier, the CE of a HWCN can be obtained by*

$$\begin{aligned}
\zeta = &\frac{1}{\sum_{k=1}^{K}\lambda_k P_k}\sum_{k=1}^{K}\lambda_k\int_{\mathbb{R}^2} e^{-\frac{\bar{\gamma}_k N_0}{P_k}\|x_{k,i_k}\|^{\alpha_k}} \\
&\times \exp\left[-2\pi^2\sum_{m=1}^{K}\lambda_m\frac{\csc\left(\frac{2\pi}{\alpha_m}\right)}{\alpha_m}\left(\bar{\gamma}_k\frac{P_m}{P_k}\right)^{\frac{2}{\alpha_m}}\right] dx_{k,i_k}.
\end{aligned} \quad (15)$$

Proof: Let us consider the k-th tier, $k = 1, 2, \ldots, K$. Since the propagation media are homogeneous, we have $\alpha_{i_1} = \alpha_{i_2} = \cdots = \alpha_{i_k} = \alpha_k$. Also, the cell density and transmission power with respect to propagation environment should also be equally allocated in the k-th tier, i.e. $\lambda_{k,i_1} = \lambda_{k,i_2} = \cdots = \lambda_{k,L_k} = \lambda_k/L_k$ and $P_{k,i_1} = P_{k,i_2} = \cdots = P_{k,L_k} = P_k$. Replacing α_{i_k} by α_k in (14), we can deduce (15). This completes the proof. □

4 Proposed Optimisation Problem for Maximising Coverage Efficiency

Intuitively, power and cell density of cells have remarkable impacts on the coverage of a practical HWCN where different propagation environments may coexist within a single cell. In particular, it can be noticed that increasing power of BSs with higher cell density does not always provide a higher coverage region. This is due to the fact that such increase of power and cell density also causes increased interferences amongst cells. Furthermore, the limited resource needs to be taken into account in the practical HWCNs. This accordingly motivates us to optimise the CE metric which is defined in (5).

Given limited power of cells and the total power available in the network, we aim at maximising the coverage with a minimum resource in terms of power consumption. In other words, we can equivalently maximise the CE of the HWCN, and hence an OP can be formulated as

$$\max_{\{\lambda_{k,i_k}\},\{P_{k,i_k}\}} \zeta \quad (16)$$

subject to the following constraints:

$$(C1): P_T \le P_{T,\max} \quad (17)$$

$$(C2): P_{k,i_k} \le P_{k,\max}, \forall k = 1, 2, \ldots, K, i_k = 1, 2, \ldots, |L_k| \quad (18)$$

where $P_{T,\max}$ and $P_{k,\max}$ denote the maximum total power available in the network and the maximum power available of cells in the k-th tier, respectively.

Notice that the CP can be determined numerically by using (13); however, it is hard to directly solve the OP in (16) given the constraints (C1) and (C2), especially when considering the practical HWCN over variant environment. Therefore, in this paper, we propose a two-stage solution including:

- *Stage 1 - Cell Density Allocation (CDA)*: This stage optimises the cell density so as to maximise the coverage region in the practical HWCN with the maximum power available at cells.
- *Stage 2 - Power Allocation (PA)*: Given the optimal cell density from Stage 1, this stage finds the optimal transmission power of BSs in different cells to minimise the total power consumption in the network while maintaining the maximum coverage.

By employing the above two stages, a maximum CE can be achieved providing a maximum coverage with a minimum total power consumption. These two stages will be described in details in the following sections.

5 Stage 1 - Cell Density Allocation

In this stage, we find the optimal CDA for maximising the coverage region in the practical HWCN subject to the limited power in the network. An OP for the CDA can be thus formulated as

$$\max_{\{\lambda_{k,i_k}\}} \mathcal{P}_C \tag{19}$$

s.t.

$$(C1'): \sum_{k=1}^{K}\sum_{i_k=1}^{L_k} \lambda_{k,i_k} P_{k,\max} \leqslant P_{T,\max}. \tag{20}$$

Notice that constraint (C1') is different from (C1) in (17) where cells at the k-th tier, in this stage, are allocated with a maximum power, i.e. $P_{k,\max}$ identified by (C2) in (18).

Another notice is that a larger coverage can be obtained when allocating higher cell density in the environment suffering higher path loss [16]. Without loss of generality, the path loss of the propagation models in the k-th tier cells, $k = 1, 2, \ldots, K$, is assumed to be in an increased order as $\alpha_{k,i_k} \leqslant \alpha_{k,i_k+1}$, where $i_k = 1, 2, \ldots, L_k - 1$. In order to achieve the maximum coverage, in addition to constraint (C1'), let us introduce the following constraint:

$$(C3): 0 < \lambda_{k,i_k} \leqslant \lambda_{k,i_k+1} \leqslant \lambda_{k,\max}, \tag{21}$$

where $\lambda_{k,\max}$ is the maximum cell density at the k-th tier in the HWCN.

In order to solve the OP in (19) subject to the constraints (C1') and (C3) in (20) and (21), respectively, due to the complexity of the derived CP, a heuristic algorithm can be employed to approximately find the optimal CDA with the following assumption:

- The density of cells at the k-th tier, $k = 1, 2, \ldots, K$, is within a set $\mathfrak{D}_k$ which includes all available cell density allocation in that tier.
- The elements in set $\mathfrak{D}_k$ can either follow a uniform distribution in the range $[0, \lambda_{k,\max}]$ or a specific setting of cells in the HWCN, e.g. with a fixed step size of $\lambda_{k,step}$.

Let $\mathcal{P}_{C,\max}^{(1)}$ and $P_T^{(1)}$ denote the maximum CP and total power consumption obtained after Stage 1, respectively, The heuristic CDA algorithm is summarised in Algorithm 1 where we first generate the whole permutation set of all available cell densities in set $\mathfrak{D}$ satisfying the constraint (C3) in (21) and then we find the set that maximises $\mathcal{P}_C$.

Algorithm 1 Heuristic CDA algorithm in Stage 1

$\mathcal{P}_{C,\max}^{(1)} \leftarrow 0$
$j_{\max} \leftarrow 0$
for $k = 1$ to K **do**
  Find $\mathfrak{G}_k \leftarrow$ all permutations of set $\mathfrak{D}_k$ satisfying (C3)
end for
$\mathfrak{G} \leftarrow \{\mathfrak{G}_1, \mathfrak{G}_2, \ldots, \mathfrak{G}_K\}$
for $j = 1$ to $|\mathfrak{G}|$ **do**
  $P_T[j] \leftarrow \sum_{k=1}^{K}\sum_{i_k=1}^{L_k}[\lambda_{k,i_k}]_j P_{k,\max}$
  if $P_T[j] \leqslant P_{T,\max}$ (see (C1')) **then**
    Find $\mathcal{P}_C$ using (13) (see the proof of Theorem 1)
    if $\mathcal{P}_C \geq \mathcal{P}_{C,\max}$ **then**
      $\mathcal{P}_{C,\max}^{(1)} \leftarrow \mathcal{P}_C$
      $j_{\max} \leftarrow j$
    end if
  end if
end for
Output:
Optimal CDA: $\{\lambda_{k,i_k}^{(opt)}\} = \{[\lambda_{k,i_k}]_{j_{\max}}\}$
Maximum CP in Stage 1: $\mathcal{P}_{C,\max}^{(1)}$
Total power consumption in Stage 1: $P_T^{(1)} = P_T[j_{\max}]$

6 Stage 2 - Power Allocation

This stage aims at minimising the total power consumption in the network subject to a coverage requirement which was determined in Stage 1, i.e. $\mathcal{P}_{C,\max}^{(1)}$, with an optimal CDA, i.e. $\{\lambda_{k,i_k}^{(opt)}\}$, $k = 1, 2, \ldots, K$, $i_k = 1, 2, \ldots, L_k$. The total power consumption in the network in Stage 2 can be thus given by

$$P_T' = \sum_{k=1}^{K}\sum_{i_k=1}^{L_k} \lambda_{k,i_k}^{(opt)} P_{k,i_k}. \tag{22}$$

Accordingly, the OP for PA can be formulated as

$$\min_{\{P_{k,i_k}\}} P_T' \tag{23}$$

s.t. (C2) in (18),

$$(C1''): P_T' \leq P_{T,\max} \tag{24}$$

$$(C4): \mathcal{P}_C \geq \mathcal{P}_{C,\max}^{(1)} \tag{25}$$

where $k = 1, 2, \ldots, K$, $i_k = 1, 2, \ldots, L_k$, and $\mathcal{P}_{C,\max}^{(1)}$ is the maximum CP determined in Stage 1.

Applying the same approach as in Stage 1, a heuristic algorithm can be employed to approximately solve the PA in (23) by assuming:

- The power level of cells at tiers can be varied within a set $\mathfrak{P}$ which contains all available cell power levels.
- The elements in set $\mathfrak{P}$ are in the range $(0, P_{k,\max}]$. They can be either uniformly distributed or provided with a specific power allocation range for a typical cell.

The heuristic PA algorithm is summarised in Algorithm 2 where constraints (C2), (C1") and (C4) are taken into account in minimising the total power consumption. Here, the CP and the minimum total power consumption obtained in Stage 2 are denoted by $\mathcal{P}_C^{(2)}$ and $P_{T,\min}^{(2)}$, respectively.

Remark 1 (Complexity Analysis)**.** Let us investigate the computational complexity, which is measured by the number of computations performed in both CDA and PA algorithms. As shown in Algorithm

Algorithm 2 Heuristic PA algorithm in Stage 2

Find $\mathfrak{P}_{\mathfrak{A}} \leftarrow$ all permutations of set $\mathfrak{P}$ satisfying (C2).
$P_{T,\min} \leftarrow 0$
$j_{\min} \leftarrow 0$
for $j = 1$ to $|\mathfrak{P}_{\mathfrak{A}}|$ **do**
  Find $\mathcal{P}_C$ using (13)
  if $\mathcal{P}_C \geq \mathcal{P}_{C,\max}^{(1)}$ (see (C4)) **then**
    $P'_T[j] \leftarrow \sum_{k=1}^{K} \sum_{i_k=1}^{L_k} \lambda_{k,i_k}^{(opt)} [P_{k,i_k}]_j$
    if $P'_T[j] \leq P_{T,\max}$ (see (C1")) **then**
      $P_{T,\min} \leftarrow P'_T$
      $j_{\min} \leftarrow j$
      $P_{T,\max} \leftarrow P_{T,\min}$
      $\mathcal{P}_C^{(2)} \leftarrow \mathcal{P}_C$
    end if
  end if
end for

Output:
Optimal PA: $\{[P_{k,i_k}]_{j_{\min}}\}$
CP in Stage 2: $\mathcal{P}_C^{(2)}$
Minimum total power consumption in Stage 2:
$P_{T,\min}^{(2)} = P'_T[j_{\min}]$

1, the number of permutations of cell density in a set $\mathfrak{G}_k$, $k = 1, 2, \ldots, K$, of the k-th tier is $|\mathfrak{D}_k|^{L_k}$. Therefore, the maximum number of executed operations for finding the optimal CDA over K tiers is $\prod_{k=1}^{K} |\mathfrak{D}_k|^{L_k}$ (i.e. the worst case until achieving the maximum CP). Similarly, the maximum number of operations in Algorithm 2 for finding the optimal PA is $\prod_{k=1}^{K} |\mathfrak{P}|^{L_k}$. In summary, the total number of operations in both stages does not exceed $\prod_{k=1}^{K} |\mathfrak{D}_k|^{L_k} + \prod_{k=1}^{K} |\mathfrak{P}|^{L_k}$.

7 Numerical Results

In this section, we first show the impacts of various parameters on the CP of an HWCN. Specifically, the CDA, PA, the number of tiers and the propagation models are consecutively considered with different sets of values to reflect the practical HWCN. The optimal CDA for maximising the CP in Stage 1 of the proposed algorithm is then presented, followed by the whole optimisation process with two stages to maximise the CE of the overall system.

7.1 Impacts of Cell Density Allocation

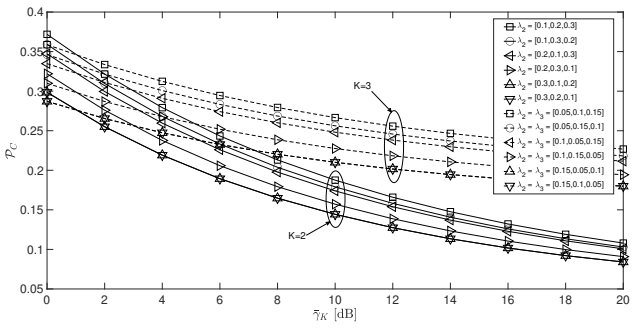

Fig. 2: CP versus SINR threshold w.r.t. cell densities in different tiers.

Figure 2 illustrates the impacts of CDA on the CP, i.e. $\mathcal{P}_C$, which is plotted as a function of the SINR threshold at the tiers, i.e. $\bar{\gamma}_K$. Two scenarios with two and three tiers in the HWCN, i.e. $K = 2$ and $K = 3$, are considered, each of which has three different kinds of propagation models, i.e. $L_1 = L_2 = L_3 = 3$, having path loss exponent in the set of $\{2.1, 2.6, 3\}$. The PA at the cells in different tiers is assumed to be $P_1 = 30$ W for macrocells and $P_2 = P_3 = 1$ W for microcells. Different sets of CDA with respect to the three propagation models are depicted for all microcell tiers except the CDA in the macrocell tier which is fixed to be 0.01 for all propagation models. For fair comparison, the densities of the microcells in the scenario of $K = 3$ are set to be a half of those in the second tier when $K = 2$. It can be observed in Fig. 2 that the CP in general decreases with a stricter QoS requirement reflected through a higher SINR threshold value. A higher cell density allocated for the model having higher path loss is shown to improve the CP when compared to the other cases. Specifically, the highest CP is achieved with $\lambda_2 = [0.1, 0.2, 0.3]$ when $K = 2$ and $\lambda_2 = \lambda_3 = [0.05, 0.1, 0.15]$ when $K = 3$. Furthermore, it is shown that, given same total of CDA, a higher coverage can be achieved by employing more tiers of microcells.

7.2 Impacts of Power Allocation

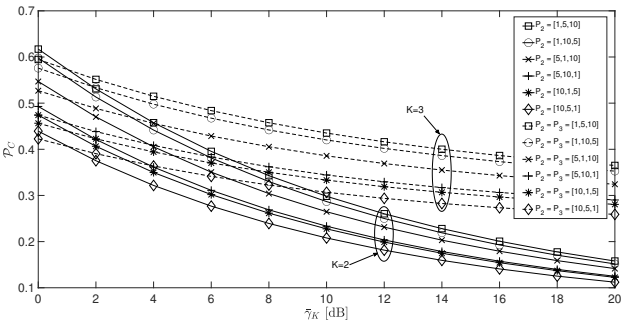

Fig. 3: CP versus SINR threshold w.r.t. PA in different tiers.

Investigating the impacts of PA on the performance of HWCN, Fig. 3 plots the CP against the SINR threshold with different sets of power at micro-cell tiers. Similarly, three propagation models, i.e. $L = 3$, having path loss exponent of $\{2.1, 2.6, 3\}$ are considered for two scenarios of $K = 2$ and $K = 3$. The densities of the microcells in each tier corresponding to $K = 2$ and $K = 3$ are assumed to be $[0.1, 0.2, 0.3]$ and $[0.05, 0.1, 0.15]$, respectively, and the density of the macrocells is 0.01 for all propagation models. The PA for the macrocells in the first tier is set as $P_1 = 30$ W, while the PA of the microcells in the remaining tiers varies as sketched in Fig. 3. It can be seen that the PA in different propagation models has a remarkable impact on the CP which is due to the different path loss exponents and cell densities in each tier. Also, a higher coverage is expected with the deployment of more microcell tiers. A further observation is that, in order to achieve a target SINR threshold, different PA can be employed with respect to the CDA, which accordingly results in different total power consumption and CP. Therefore, it is crucial to optimise both the PA and CDA so as to obtain an acceptable CP with a minimum total power, or a maximum CP with a low power supply.

7.3 Impacts of Propagation Models

The impacts of propagation models on the performance of an HWCN is illustrated in Fig. 4 where the CP is plotted versus the SINR threshold with respect to the distribution of propagation models in different tiers. Similar to Figs. 2 and 3, two cases of two-tier and three-tier HWCN, i.e. $K = 2$ and $K = 3$, are considered, each of which has up to three propagation models, i.e. $L \leq 3$, depending on their model distribution. Specifically, in Fig. 4, a binary matrix $\mathbf{B}$ of length $K \times L$ is used to indicate the existence of the propagation models in different tiers in which the row and column indices represent the level of tiers and the type of propagation models, respectively. The path loss exponents of these three models if existing are assumed

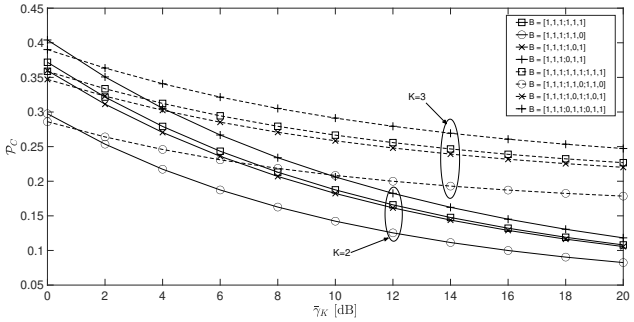

Fig. 4: CP versus SINR threshold w.r.t. propagation models in different tiers.

to be in the ordered set $\{2.1, 2.6, 3\}$. The PA for macrocells and microcells are 30 W and 1 W, respectively. The density of macrocells is 0.01 in all propagation models and the total density of microcells in all tiers, for fair comparison, are equally set to be 0.6 irrespective of the building distribution. It can be observed in Fig. 4 that the CPs of the scenarios $\mathbf{B} = [1, 1, 1; 0, 1, 1]$ when $K = 2$ and $\mathbf{B} = [1, 1, 1; 0, 1, 1; 0, 1, 1]$ when $K = 3$ are the highest, while the scenarios $\mathbf{B} = [1, 1, 1; 1, 1, 0]$ and $\mathbf{B} = [1, 1, 1; 1, 1, 0; 1, 1, 0]$ have a lowest CP. For that reason, the propagation environment has a significant impact on the practical implementation of the HWCN where the data transmission is mainly carried out in variant models and distributions.

7.4 Impacts of the Number of Tiers

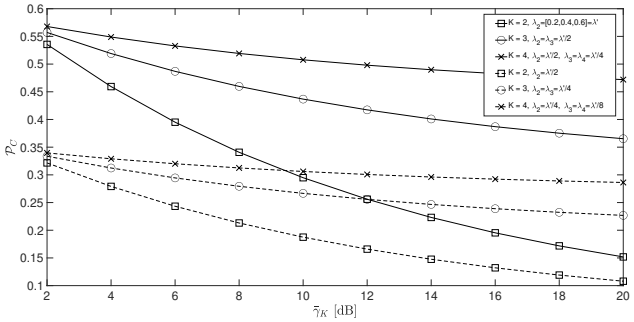

Fig. 5: CP versus SINR threshold w.r.t. number of tiers and different CDA.

Taking into account diverse tiers in an HWCN, Fig. 5 plots the CP as a function of the SINR threshold with respect to three cases of the number of tiers, i.e. $K = \{2, 3, 4\}$. Different densities of mciro-cells are also considered for each case with the same settings of other parameters as in Fig. 2, i.e. $\alpha \in \{2.1, 2.6, 3\}$, $P_1 = 30$ W and $P_2 = P_3 = P_4 = 1$ W. The CDA in the microcell tiers is assigned by splitting equally the higher-order tier, i.e. the third tier is formed by splitting the second layer into half and then the fourth layer is formed by splitting the third tier also into half. As can be seen in Fig. 5, the CP can be significantly enhanced with tier splitting, which again reveals the benefit of employing the microcells in the HWCN.

7.5 Optimal CDA in HWCN

Given the above observations of various impacts of propagation environment on the performance of HWCN, this subsection introduces the first stage of the developed OP to find the optimal CDA to maximise the CP subject to the constraints on the total power consumption. Figs. 6 and 7 sequentially plot the CP and the corresponding required power as functions of the maximum total power

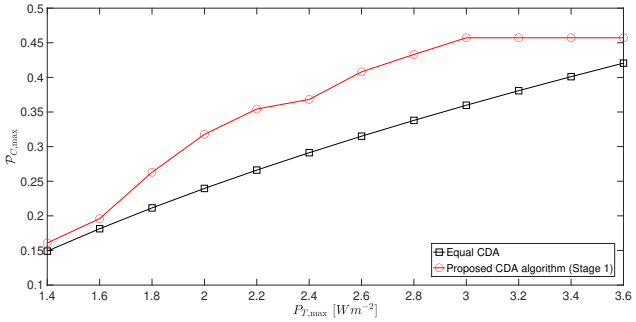

Fig. 6: CP versus maximum total power with CDA optimisation.

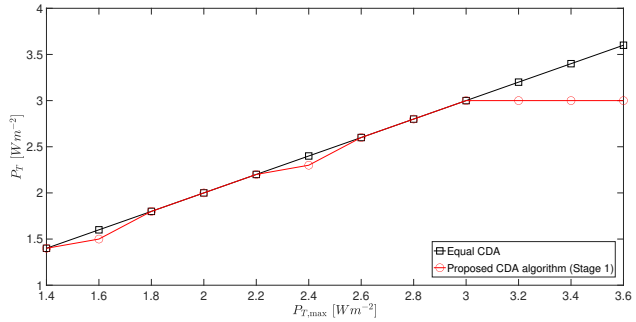

Fig. 7: Total required power versus maximum total power with CDA optimisation.

available in the network. The simulation parameters are similarly set as in Fig. 2 for the scenario of two tiers, i.e. $K = 2$, $L = 3$, $\alpha \in \{2.1, 2.6, 3\}$, $P_1 = 30$ W and $P_2 = 1$ W. For comparison, the conventional method with equal CDA is considered where all cells are allocated with the same density regardless of the propagation environment. It can be observed in Fig. 6 that a higher CP is achieved with the proposed heuristic CDA algorithm when compared to the equal CDA. A further observation in Fig. 7 is that the proposed CDA requires a lower power than the conventional approach.

7.6 Two-Stage Resource Allocation for Maximising CE

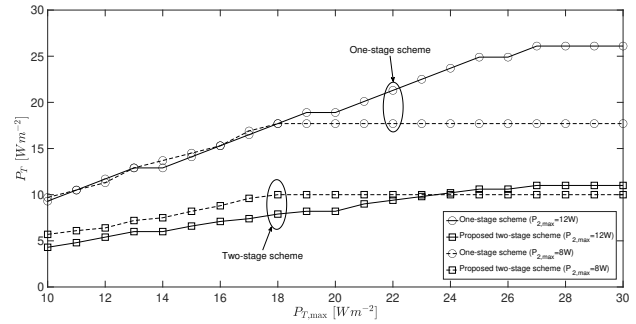

Fig. 8: Total required power versus maximum total power with one-stage and two-stage optimisation schemes.

Implementing both stages of the developed OP to maximise the overall CE in an HWCN, Figs. 8, 9 and 10 sequentially plot the total required power, i.e. P_T, the CP, i.e. $\mathcal{P}_C$, and the corresponding CE, i.e. ζ, versus the total power available in the network, i.e. $P_{T,\max}$. For comparison, both one-stage and two-stage OPs are considered with $K = 2$, $L = 3$ and $\alpha \in \{2.1, 2.6, 3\}$. The power allocated for macrocells is fixed as $P_1 = 30$ W, while two sets of the maximum

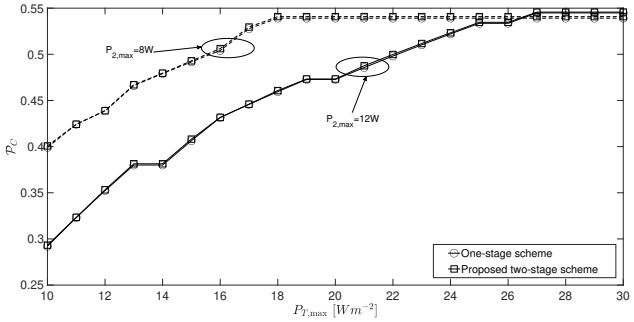

Fig. 9: CP versus maximum total power with one-stage and two-stage optimisation schemes.

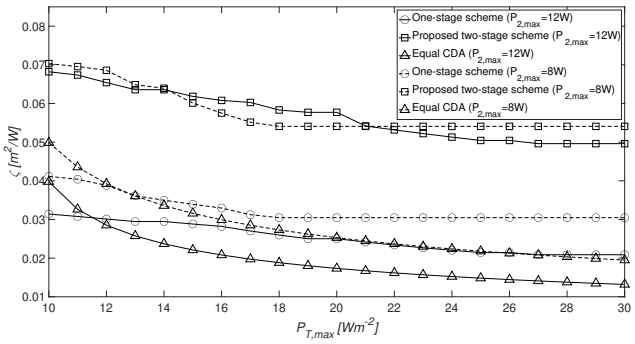

Fig. 10: CE versus maximum total power.

power of microcells in the second tier, i.e. $P_{2,\max}$, are taken into account with $P_{2,\max} = \{8, 12\}$ W.

As shown in Fig. 8, the total required power in the proposed two-stage approach is much lower than that with the one-stage scheme when the maximum CP is the only objective. It can be further observed that the required power for $P_{2,\max} = 8$ W is higher than that for $P_{2,\max} = 12$ W in case of low $P_{T,\max}$, otherwise less power is required when $P_{2,\max} = 8$ W. This is on account of the fact that a higher cell density is allocated to achieve a larger coverage when the power of cells in a tier is low, and thus more power is required when $P_{2,\max} = 8$ W. On the other hand, a higher cell power may reduce the coverage due to the interference, and for this reason, lower cell density with less power is allocated when $P_{2,\max} = 12$ W and $P_{T,\max}$ is low. When $P_{T,\max}$ increases, more power can be supplied for the cells having $P_{2,\max} = 12$ W; however, this is restricted for those having $P_{2,\max} = 8$ W. In addition, the CP of the two-stage approach in Fig. 9 is shown to be the same as with only one stage since the second stage of the OP only requires to satisfy a minimum CP which was found in the first stage. This accordingly results in an enhanced overall CE in Fig. 10 with the proposed two-stage algorithm compared to the one-stage algorithm and the conventional approach with equal CDA at all building types. Specifically, the two-stage algorithm achieves the CE of up to 1.5 times and 2.5 times higher than that in the one-stage algorithm and the equal CDA, respectively. Furthermore, it can be seen in Fig. 10 that the CE fluctuates when the maximum cell power varies. This is owing to the fact that ζ is proportional to $\mathcal{P}_C$, but it is inversely proportional to P_T; however, as shown in Figs. 8 and 9, both $\mathcal{P}_C$ and P_T are shown to vary non-monotonically with respect to $P_{2,\max}$ in certain range of $P_{T,\max}$.

8 Conclusions

In this work, we have first conducted studies on the impacts of PA and CDA on the CE of a downlink HWCN taking into account various propagation environment. Then, we have formulated an OP to maximize the CE by optimizing the PA and CDA for HWCN under the constraints of limited power at cells and total power available in the network. A two-stage approach for solving the OP has been proposed to sequentially obtain the heuristic value of the CDA and PA. The heuristic solution has been shown to significantly enhance the CE of up to 1.5 times and 2.5 times compared to the one-stage algorithm and the equal CDA, respectively. The future work would be the investigation of the CE in the practical HWCNs when the number of BSs in different tiers and different environment can vary over time, which can be modelled by a nonstationary PPP. Moreover, the scenario when the BSs can collaborate with each other will be considered, where the cells are clustered following Poisson cluster process.

9 References

1 A. Damnjanovic, J. Montojo, Y. Wei, T. Ji, T. Luo, M. Vajapeyam, T. Yoo, O. Song, and D. Malladi, "A survey on 3GPP heterogeneous networks," *IEEE Wireless Commun.*, vol. 18, no. 3, pp. 10–21, Jun. 2011.

2 J. Andrews, "Seven ways that HetNets are a cellular paradigm shift," *IEEE Commun. Mag.*, vol. 51, no. 3, pp. 136–144, Mar. 2013.

3 Y. Li, Y. Zhang, K. Luo, T. Jiang, Z. Li, and W. Peng, "Ultra-dense HetNets meet big data: Green frameworks, techniques, and approaches," *IEEE Commun. Mag.*, vol. 56, no. 6, pp. 56–63, 2018.

4 H. Q. Tran, C. V. Phan, and Q.-T. Vien, *An Overview of 5G Technologies*. Singapore: Springer Singapore, 2018, pp. 59–80.

5 W. Chien, H. Cho, C. Lai, F. Tseng, H. Chao, M. M. Hassan, and A. Alelaiwi, "Intelligent architecture for mobile HetNet in B5G," *IEEE Netw.*, vol. 33, no. 3, pp. 34–41, 2019.

6 C.-L. I, L. J. Greenstein, and R. D. Gitlin, "A microcell/macrocell cellular architecture for low- and high-mobility wireless users," *IEEE J. Sel. Areas Commun.*, vol. 11, no. 6, pp. 885–891, Aug. 1993.

7 X. Lagrange, "Multitier cell design," *IEEE Commun. Mag.*, vol. 35, no. 8, pp. 60–64, Aug. 1997.

8 E. Ekici and C. Ersoy, "Multi-tier cellular network dimensioning," *ACM Wireless Netw.*, vol. 7, no. 4, pp. 401–411, Sep. 2001.

9 J. Andrews, H. Claussen, M. Dohler, S. Rangan, and M. Reed, "Femtocells: Past, present, and future," *IEEE J. Sel. Areas Commun.*, vol. 30, no. 3, pp. 497–508, Apr. 2012.

10 R. Trestian, Q.-T. Vien, P. Shah, and G. E. Mapp, "Exploring energy consumption issues for multimedia streaming in LTE HetNet small cells," in *Proc. IEEE LCN 2015*, Florida, USA, Oct. 2015, pp. 498–501.

11 R. Trestian, Q.-T. Vien, P. Shah, and G. Mapp, "UEFA-M: Utility-based energy efficient adaptive multimedia mechanism over LTE HetNet small cells," in *Proc. ISWCS 2017*, Aug 2017, pp. 408–413.

12 H. Gu, H. Inaltekin, and B. S. Krongold, "Coverage modelling and handover analysis in ultra-dense heterogeneous networks," in *Proc. IEEE ICC 2019*, 2019, pp. 1–6.

13 N. Arulselvan, V. Ramachandran, S. Kalyanasundaram, and G. Han, "Distributed power control mechanisms for HSDPA femtocells," in *Proc IEEE VTC-Spring 2009*, Barcelona, Spain, Apr. 2009, pp. 1–5.

14 X. Li, L. Qian, and D. Kataria, "Downlink power control in co-channel macrocell femtocell overlay," in *Proc. CISS'09*, Baltimore, Maryland, USA, Mar. 2009, pp. 383–388.

15 M. Shaat and F. Bader, "A two-step resource allocation algorithm in multicarrier based cognitive radio systems," in *Proc. IEEE WCNC 2010*, Sydney, Australia, Apr. 2010, pp. 1–6.

16 Q.-T. Vien, T. Akinbote, H. X. Nguyen, R. Trestian, and O. Gemikonakli, "On the coverage and power allocation for downlink in heterogeneous wireless cellular networks," in *Proc. IEEE ICC 2015*, London, UK, Jun. 2015, pp. 4641–4646.

17 Q.-T. Vien, T. A. Le, H. X. Nguyen, and M. Karamanoglu, "An energy-efficient resource allocation for optimal downlink coverage in heterogeneous wireless cellular networks," in *Proc. IEEE ISWCS 2015*, Brussels, Belgium, Aug. 2015, pp. 156–160.

18 X. Jiang and F.-C. Zheng, "User rate and power optimization for HetNets under Poisson cluster process," *EURASIP J. Wireless Commun. Netw.*, vol. 2019, no. 1, p. 237, 2019.

19 J. Andrews, F. Baccelli, and R. Ganti, "A tractable approach to coverage and rate in cellular networks," *IEEE Trans. Commun.*, vol. 59, no. 11, pp. 3122–3134, Nov. 2011.

20 H. ElSawy, E. Hossain, and M. Haenggi, "Stochastic geometry for modeling, analysis, and design of multi-tier and cognitive cellular wireless networks: A survey," *IEEE Commun. Surveys Tuts.*, vol. 15, no. 3, pp. 996–1019, Third 2013.

21 J. Chen and C. Yuan, "Coverage analysis of user-centric wireless network in a comprehensive fading environment," *IEEE Commun. Lett.*, vol. 22, no. 7, pp. 1446–1449, 2018.

22 M. Haenggi, J. Andrews, F. Baccelli, O. Dousse, and M. Franceschetti, "Stochastic geometry and random graphs for the analysis and design of wireless networks," *IEEE J. Sel. Areas Commun.*, vol. 27, no. 7, pp. 1029–1046, Sep. 2009.

23 F. Baccelli and B. Baszczyszyn, *Stochastic Geometry and Wireless Networks*. NOW: Foundations and Trends in Networking, 2010, vol. 3, no. 3-4.

24 S. N. Chiu, D. Stoyan, W. S. Kendall, and J. Mecke, *Stochastic Geometry and Its Applications*, 3rd ed. John Wiley and Sons, 2013.

25 Z. Gong and M. Haenggi, "Interference and outage in mobile random networks: Expectation, distribution, and correlation," *IEEE Trans. Mobile Comput.*, vol. 13, no. 2, pp. 337–349, Feb 2014.

26 H. Dhillon, R. Ganti, F. Baccelli, and J. Andrews, "Modeling and analysis of K-tier downlink heterogeneous cellular networks," *IEEE J. Sel. Areas Commun.*, vol. 30, no. 3, pp. 550–560, Apr. 2012.
27 C. Ma, M. Ding, D. Lopez-Perez, Z. Lin, J. Li, and G. Mao, "Performance analysis of the idle mode capability in a dense heterogeneous cellular network," *IEEE Trans. Commun.*, vol. 66, no. 9, pp. 3959–3973, Sep. 2018.
28 Y. Li, H. Zhang, J. Wang, B. Cao, Q. Liu, and M. Daneshmand, "Energy-efficient deployment and adaptive sleeping in heterogeneous cellular networks," *IEEE Access*, vol. 7, pp. 35 838–35 850, 2019.
29 R. Tao, W. Liu, X. Chu, and J. Zhang, "An energy saving small cell sleeping mechanism with cell range expansion in heterogeneous networks," *IEEE Trans. Wireless Commun.*, vol. 18, no. 5, pp. 2451–2463, May 2019.
30 I. S. Gradshteyn and I. M. Ryzhik, *Table of Integrals, Series, and Products*, 7th ed. Academic Press, 2007.